STATISTICAL MORPHOMETRY OF SMALL MARTIAN CRATERS: NEW METHODS AND RESULTS

W. A. Watters[1], L. Geiger[1,2], M. Fendrock[1], R. Gibson[1], and A. Radford[1]. [1]Dept. of Astronomy, Whitin Observatory, Wellesley College (wwatters@wellesley.edu), [2]now at Massachusetts Institute of Technology, Man-Vehicle Lab

Introduction: We present results from recent and ongoing work [e.g., 1, 2] that examines the distribution of small crater shapes on Mars (30 m < D < 5 km), as well as an evaluation of stereo-derived digital elevation models (DEMs) generated using a new tool suite (Ames Stereo Pipeline [3]). We also describe computational methods developed in-house for automatically characterizing crater shape for large statistical studies [4].

Our goals are to examine the dependence of crater morphometry upon impact parameters such as (a) target material properties; (b) impact velocity (estimated for secondary craters); and (c) the role of planetary gravity (e.g., size-dependent transitions). With the advent of high-resolution imagery and elevation models, fine-scale features (~10 m scale) of crater shape can now be used to examine important transitions that depend on all three factors: e.g., the strength-to-gravity transition, the simple-to-complex transition (and "precursors" at smaller diameters), the splash-to-explosion transition, and the "Odessa-to-Barringer transition" [5].

By comparing fine-scale morphometry of craters that have undergone varying degrees of modification, we have begun to characterize the modification sequence for martian craters in multiple environments.

Elevation models: Although recent work has begun making use of highest-resolution imagery [e.g., 6], most morphometric studies of the past 1.5 decades have relied on elevation data from laser altimetry and stereo-derived DEMs at coarser resolutions than we examine here [e.g., 7,8,9]. A portion of our analyses rely heavily on DEMs derived from stereo HiRISE observations (High Resolution Imaging Science Experiment on the Mars Reconnaissance Orbiter [10]). Absolute validation of these models is difficult because only rover imagery is resolved at higher resolutions, and has limited coverage.

The Ames Stereo Pipeline (ASP) has placed the production of elevation models within reach of all planetary scientists at zero cost by means of open source tools [4]. We have evaluated ASP-derived products by comparing our own ASP models to models generated by the HiRISE Science Team using the proprietary SOCET SET (SS) tool suite [11]. We compared the models of 20 impact craters from 12 image pairs by subtracting 360 radial elevation profiles of each ASP model from their counterparts in corresponding SS models.

The ASP models were not bundle-adjusted or tied to MOLA topography because these steps do not influence relative model elevations at small scales. We do not use interpolated elevations in our measurements of morphometric quantities (except cavity volume). Craters were localized for comparison by first extracting the crater rim trace using automatic methods (see below), and then computing a centroid.

We find that individual elevations in the ASP models deviate from the published HiRISE team models by < 0.5 m on average. These results are encouraging for the use of ASP to generate DEMs for studies of the statistical morphometry of small-scale topographic features on Mars.

Methods: We have developed a library of Python programs that can be used to characterize impact craters in an automatic way, requiring human intervention to fix errors in less than 5-10% of cases, depending on the crater population [3]. First, the user selects an approximate crater center and two points on the rim to estimate an approximate initial position and radius. The program then finds a candidate rim by selecting positions that correspond to the maximum elevations measured along radial elevation profiles. A plane is fit to this candidate rim and subtracted from the DEM.

The program then identifies points of interest (POIs) along radial elevation profiles as belonging to one of the following categories: slope break, radial local maximum, or radial global maximum. A program then assembles candidate rim segments from these POIs. The final rim is computed by stitching together the candidate segments while minimizing the largest radial discontinuity and maximizing the extent of overlap with the radial global-maximum elevations.

Morphometric parameters. The rim trace and elevation model are required to compute all of the following morphometric quantities: (a) cavity volume; (b) rim diameter; (c) rim-to-floor depth; (d) curvature radius of upper rim walls; (e) angular span of the crater rim; (f) crater rim and flank slopes; (g) rim height; (h) exponent of power-law fit to crater cavity cross-section; (i) azimuth to tallest rim; (j) azimuth from lowest point to centroid; (k) planform aspect ratio; (l) radial standard deviation of planform; (k) correlation between rim elevation and azimuthal radius. Since many of these quantities are measured from (non-overlapping) radial profiles ((b)-(h)), mean values are reported for the crater as a whole.

Target properties. To measure the influence of target properties, a global geologic map [12] is used to assign a geologic unit to each crater, as in [13]; units are categorized as high or low strength (e.g., crater cavities or ejecta are relatively weak; lava plains are relatively strong). The statistical distribution of impact crater parameter values are compared for different terrains using the two-sample Kolmogorov-Smirnov test to determine effects on crater shape [1].

Modification. Finally, a coarse indicator of modification state is estimated according to rubrics that are qualitative and semi-quantitative. Each crater is assigned a score that is the sum of visual hallmarks of preservation (e.g., preserved rays and absence of cavity fill). A semi-quantitative approach instead identifies craters as highly modified if they exhibit statistically low crater depths or rim heights. Using these coarse measures of modification state, we have characterized how crater shape responds to surface processes [1].

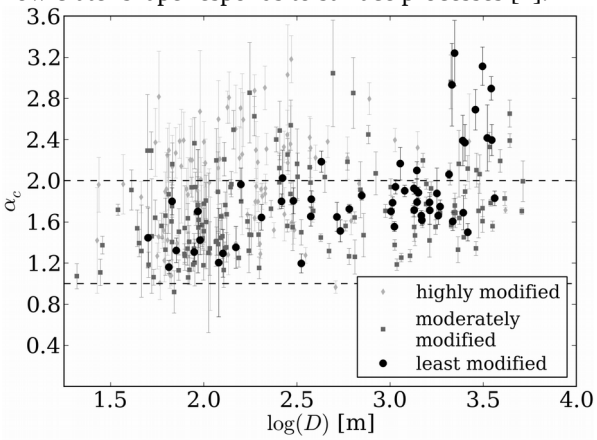

Fig. 1: Power-law cavity exponent versus diameter in the range from conical ($\alpha_c \simeq 1$) to paraboloidal ($\alpha_c \simeq 2$) and superparaboloidal ($\alpha_c > 2$). From [1].

Results: As mentioned, our goals are to characterize martian crater morphometry as a function of crater size, approximate impactor velocity (in secondary craters), target properties, and modification state. We supply two illustrative results in this abstract and refer the reader to recent and upcoming publications for details [e.g., 1,2].

Cavity shape. Fig. 1 shows the power law exponent fitted to crater cavities as a function of diameter and modification state. Small craters are closer to conical ($\alpha_c \simeq 1$) while larger craters are paraboloidal ($\alpha_c \simeq 2$) to superparaboloidal ($\alpha_c > 2$). The cavity shape exponent also tends to increase with modification. The formation of conical craters at small sizes may imply lower impact velocities and shallower explosion depths (used to account for the conical shape of expansion-dominated Odessa-style craters on Earth [5]). Paraboloidal craters have a shape more consistent with excavation-dominated Barringer-style craters [5]. Well-preserved superparaboloidal craters exhibit features of incipient crater collapse (for D ≳2.5 km).

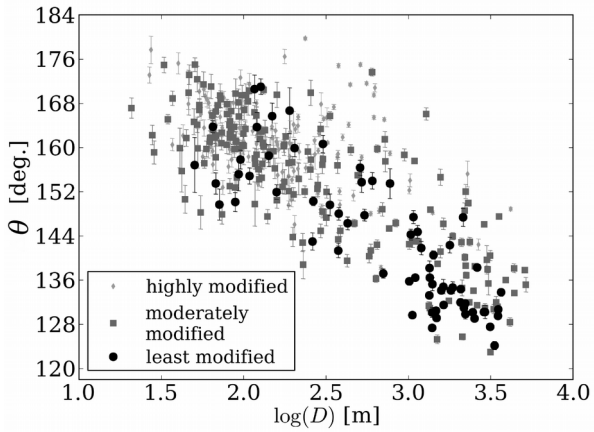

Fig. 2: Rim span (θ) vs. crater diameter: θ decreases linearly with log(D) down to typical repose angles near the simple-complex transition diameter. From [1].

Rim span. It has been known for some time that wall slopes for simple craters on the Moon steepen with increasing diameter [14]. We explore this diameter dependence in relation to the simple-complex transition and "precursor" transitions at smaller diameters.

We define the rim span (θ) as the angle between the flankward and craterward rim slopes [1]: e.g., a rim span of 180° suggests a perfectly flat rim, while a span of 120° indicates that both slopes occur in the range of typical repose angles. Fig. 2 shows that rim span decreases with diameter and crosses 120° at a diameter somewhat in excess of the simple-complex transition on Mars [9]. That is, rim and flank slopes steepen with diameter up to typical repose angles at roughly the onset diameter for crater collapse.

References: [1] Watters, W.A. et al., (2015) *JGR*, doi: 10.1002/2014JE004630; [2] Watters, W. A. and Radford, A. (2014), *LPSC 45*, #2836; [3] Moratto, Z., et al., (2010) *LPSC 41*, #2364; [4] Geiger, L., (2013) *Wellesley Honors thesis;* [5] Shoemaker et al. (2005) *Aus. J. Earth Sci.., 52* ,529-544; [6] Daubar, I. J., et al. (2014) *JGR, 119*,2620-2639; [7] Garvin, J. et al.(2000), *Icarus, 144*, 329-352; [8] Stewart, S. and Valiant, G. (2006) *Meteor. Planet Sci., 41*,1509-1537; [9] Robbins, S & Hynek, B. (2012) *JGR, 117*, E06001; [10] McEwen, A. et al., (2007) *JGR, 112*, E05S02; [11] Kirk et al., (2008) *JGR*, 113, E00A24; [12] Tanaka et al. (2014) *USGS map* #3292; [13] Whitehead, J., et al. (2010) *GSA special papers*, *465*, 67-81; [14] Pike, R.J. (1977) *Impact & Explosion Cratering*, 489-509.